Fuzzy Model Predictive Direct Torque Control of IPMSMs for Electric Vehicle Applications

Jackson John Justo, Francis Mwasilu, Eun-Kyung Kim, Jinuk Kim, Han Ho Choi, *Member, IEEE*, and Jin-Woo Jung, *Member, IEEE*

***Abstract*—This paper proposes a fuzzy model predictive direct torque control (FMP-DTC) strategy of interior permanent magnet synchronous motors (IPMSMs) for electric vehicle (EV) applications. The fuzzy logic control technique incorporated into the proposed FMP-DTC scheme dynamically determines the appropriate values of the weighting factors, and then generates the optimal switching states that minimize the electromagnetic torque and stator flux errors. Unlike the conventional model predictive (MP)-DTC strategy, the optimal switching states of the proposed FMP-DTC are selected without retuning the weighting factors. It means that they are updated depending on the specific operating conditions. Therefore, the proposed FMP-DTC is effective in various operating conditions that make it suitable for the EV-traction operating environment. Hence, the proposed FMP-DTC method has a simple control structure and can explicitly handle the system constraints. The performance evaluation is carried out via both MATLAB/Simulink and a prototype IPMSM test-bed with a TMS320F28335 digital signal processor (DSP). Comparative simulation and experimental results present the evidence of the performance improvements based on the proposed FMP-DTC strategy compared with the conventional MP-DTC strategy by indicating a fast transient torque response, low ripples, and an accurate speed tracking even under rapid climbing or emergency braking situations.**

***Index Terms*—Direct torque control (DTC), fuzzy logic control (FLC), fuzzy model predictive (FMP) control, interior permanent magnet synchronous motor (IPMSM).**

I. Introduction

INTERIOR permanent magnet synchronous motors (IPMSMs) have been considered as the potential candidates for electric vehicle (EV) applications [1] due to their compact structure with small size and weight, high torque to inertia ratio, high efficiency, wide speed range, low noise, and robust operations [2]. Focusing on the EV-traction application, a fast and robust torque response of the IPMSM drive is required to meet the instantaneous torque demand commanded by the driver through the pedal action. Moreover, the IPMSM drive should have a quick torque/speed recovery capability after subjected to sudden system disturbances. These are some of the requirements of the EV's torque/speed demand which have to be achieved to match the vehicles cruising capabilities similar to internal combustion engines (ICEs) [3].

In the literature, in order to enhance the steady-state and dynamic performances of the IPMSM drive, methods like the field-oriented control (FOC) with pulse-width modulation (PWM) are presented [4], [5]. The quality of the FOC-PWM scheme depends on the performance of the outer and inner control loops. One of the notable drawbacks of this control scheme is the limited bandwidth which leads to an unsatisfactory control performance during transient state [6]. Alternatively, a direct torque control (DTC) strategy has been proposed to improve the dynamic performance of ac machines that need fast transient responses [7], [8]. The basic principle of the conventional DTC method is to select the optimal stator voltage vectors based on the error sign between the torque and estimated stator flux linkage values and their respective commanded signals [9]. However, high torque and flux ripples can be observed, which are limited by the hysteresis bandwidth. This is undesirable performance and it is the main limitation of the conventional DTC [10].

To overcome these drawbacks, improved DTC algorithms have been reported in the literature [11]–[15]. For instance, the basic DTC strategy can be integrated with the space vector modulation (SVM) scheme [11]. Different from the conventional one, the DTC-SVM generates a random voltage vector using any amplitude and length within its linear range. In this case, the torque and stator flux are regulated more accurately with a fixed switching frequency [12], [13]. Note that, the DTC-SVM operating technique relies on how to select the firing voltage vector for a given sampling interval. Now, using deadbeat control [14], sliding mode control [15] or nonlinear optimal control [16], the DTC-SVM can be further improved to generate lower torque and stator flux ripples with fixed switching frequency. On the other hand, their constraints such as coordinate transformation, much knowledge of the motor parameters, and high computational burden, may negate their simplicity and robustness.

Manuscript received May 4, 2016; revised August 14, 2016 and December 1, 2016; accepted January 30, 2017. Date of publication February 7, 2017; date of current version August 14, 2017. This work was supported by the National Research Foundation of Korea (NRF) funded by the Korea Government [Ministry of Science, ICT, and Future Planning (MSIP)] under Grant 2015R1A2A2A01003513. Recommended by Technical Editor Sanjeet Kumar Dwivedi.

The authors are with the Division of Electronics and Electrical Engineering, Dongguk University, Seoul 04620, Korea (e-mail: jinwjung@dongguk.edu).

Color versions of one or more of the figures in this paper are available online at http://ieeexplore.ieee.org.

Digital Object Identifier 10.1109/TMECH.2017.2665670

1083-4435 © 2017 IEEE. Personal use is permitted, but republication/redistribution requires IEEE permission.
See http://www.ieee.org/publications_standards/publications/rights/index.html for more information.

Recently, model predictive control (MPC) strategy, which can take into account the plant constraints and nonlinearities with multiple inputs/outputs and handle them in a proper way, has been reported [17]–[19]. In general, the MPC scheme has a simple and optimal control structure in the sense that it minimizes the errors of the control parameters in order to select a desired switching state [17]. Thus, it can be combined with the basic DTC to form the model predictive (MP) DTC (i.e., MP-DTC) scheme that can achieve a high-performance control for the PMSM drives. Unlike the basic DTC or FOC with SVM, the MP-DTC strategy is based on the optimal control approach [18]. Having the cost function designed to minimize the torque and stator flux control errors, the optimized switching states can be generated [19]. The technique is to minimize the electromagnetic torque error (i.e., ΔT_{el}) and stator flux linkage error (i.e., $\Delta\psi_s$) by penalizing those errors using the weighting factors. However, it is not only a difficult but challenging and time-consuming problem to choose the exact values of the weighting factors at every sampling interval in order to obtain the optimized switching states [20]. In [21] and [22], the authors proposed the methods to optimize and eliminate the weighting factor in the cost function in order to generate optimal voltage vectors, respectively. Moreover, an MPC incorporating a fuzzy decision-making technique with multiple control objectives is proposed for the matrix converter whereby the weighting factor is varied to simplify the tuning process [23]. However, in an environment where it is required to accurately anticipate the future behaviors of the plant (like an EV drive) along with the time for transient-state, tuning the weighting factors for the MP-DTC scheme is still an open problem to find reliable, accurate, and optimal solutions [24].

Therefore, this paper proposes a DTC strategy based on a fuzzy model predictive (FMP) control for the EV-traction using an IPMSM drive. Given the EV system dynamics and an objective cost function, the proposed FMP-DTC strategy uses a fuzzy logic control (FLC) technique to online determine the appropriate values of the weighting factors (i.e., weighting factors). Within that perspective, the optimal switching states are applied to the IPMSM drive. By employing the proposed FMP-DTC scheme, the system complexity and constraints can be easily handled to achieve a high-performance torque control for the EV traction with the IPMSM drive. Contrary to the conventional MP-DTC which employs fixed weighting factors, the optimal switching states of the proposed FMP-DTC are chosen without retuning the weighting factors regardless of the operating conditions such as sudden external disturbance or transient speed change. As a result, the proposed FMP-DTC is very effective in various operating conditions. In this paper, the performance of the proposed scheme is validated by using both MATLAB/Simulink and a prototype IPMSM test-bed with a Texas Instrument (TI) TMS320F28335 DSP. Comparative simulation and experimental results reveal the superior performance of the proposed FMP-DTC over the conventional MP-DTC scheme such as a fast torque response, low ripples, and an accurate speed trajectory tracking even under rapid climbing or emergency braking situations.

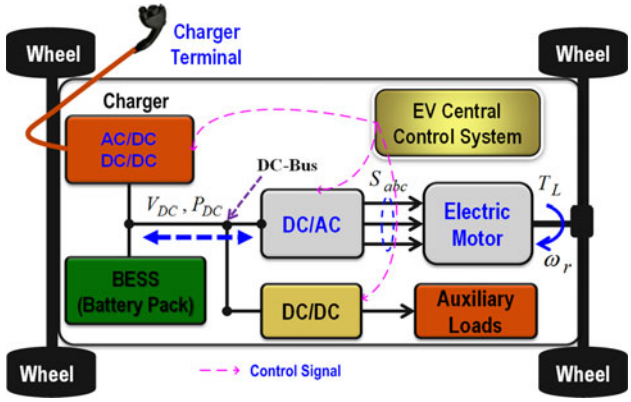


Fig. 1. Block diagram of the BEV traction with its major electrical components.

II. EV System Description, Control Requirements, and Problem Statement

A. System Descriptions and Control Requirements

Fig. 1 shows the major electrical components of the battery EV (BEV) traction as follows: 1) an electric motor drive including a three-phase inverter and a drive train; 2) battery energy storage system; 3) charging system (i.e., charging plug, ac/dc converter, and dc/dc converter); and 4) EV central control system. Now due to the specific demand operation and varying on-road conditions, the electric motor drives are required to own some special characteristics, e.g., large torque output below its base speed, high efficiency in wide speed and torque ranges, etc. [3].

In that perspective, the DTC for EV-traction applications is not a simple task in the sense that the EV operation is essentially a time-varying system (i.e., the EV parameters and road conditions are always time-varying). Actually, there are some specific factors that make the EVs' performance lag behind the ICE vehicles as follows: 1) Limited cruising range and energy-saving strategy, 2) Charging and discharging rate, powertrain efficiency, and motion maneuverability, and 3) Overall system safety/protection and ride comfort.

So, in order to close these performance gaps, the DTC scheme for EV traction with an IPMSM drive should be designed with at least the following control requirements:

1) capability to maximize the efficiency of the motor drive over the whole speed range to extend cruising mileage for starting, rapid acceleration, cornering, and emergency braking [3], [25];
2) capability to safely ride-through during complicated operating conditions, e.g., fault-tolerant control [26], [27];
3) ability to regenerate power during braking (i.e., eco-driving or regenerative braking capability), and recharge within a short time with a charge saving strategy so as to match the ICEs refueling process.

B. DTC Problem Statement Based on Predictive Control

In a precalculating process such as an EV-traction, driver's decision optimization at every time instant is paramount, i.e.,

during acceleration, overtaking, and or braking according to the driving conditions. Likewise, in a real driving environment, some different conditions may require a variable load torque demand which is realizable by the accelerator pedal action. Thus, the driving torque control action requires an adaptive controller which can instantly obeys the drivers' online torque requirements. In this case, the MP-DTC has been proposed in the literature to serve this purpose. In the MP-DTC scheme, the weighting factors highly influence the torque and stator flux ripples for the same sampling frequency set [21]–[24]. For instance, if the torque errors are big or large, then the weighting factors should make them (errors) weigh more to reduce their influence on voltage selection and the converse is true for the voltage selection on small torque errors. Note that the minimum error has a high priority in selecting the switching states. Thus, it is difficult to guarantee the high-performance over various operating conditions by applying fixed weighting factors like in the conventional MP-DTC.

Therefore, to improve the performance of the EV traction, the DTC scheme should be designed with adaptive properties. It should also be able to handle all difficulties in covering a real-world with a set of possible individual driving situations like torque or speed change. Hence, the MPC scheme intuitively resembles a human physiological control, has simple structure and ability to deal with various system constraints [24]. In this case, a FMP-DTC scheme is proposed in this paper. The proposed scheme introduces variable weighting factors which are tuned by the FLC technique to minimize the errors between the predicted torque and stator flux linkage values and their respective reference signals.

III. FMP-DTC Design

A. Dynamic Model of an IPMSM Drive

To design the FMPC strategy, the dynamic model of a three-phase IPMSM drive in the *d–q* rotor rotating reference frame can be expressed as [2]

$$\begin{aligned}\dot{\omega}_r &= Z_1 i_q - Z_2\omega_r - Z_3 T_L + Z_9 i_q i_d\\ \dot{i}_q &= -Z_4 i_q - Z_5\omega_r + Z_6 u_q - Z_{10}\omega_r i_d\\ \dot{i}_d &= -Z_7 i_d + Z_8 u_d + Z_{11}\omega_r i_q\end{aligned} \tag{1}$$

where the variables Z_1 to Z_{11} are obtained in terms of their physical motor parameters as

$$Z_1 = \frac{3}{2}\times\frac{1}{J_m}\times\frac{p^2}{4}\times\psi_m,\ Z_2 = \frac{B_m}{J_m},\ Z_3 = \frac{p}{2J_m},$$
$$Z_4 = \frac{R_s}{L_q},\ Z_5 = \frac{\psi_m}{L_q},\ Z_6 = \frac{1}{L_q},\ Z_7 = \frac{R_s}{L_d},\ Z_8 = \frac{1}{L_d},$$
$$Z_9 = \frac{p\,(L_d - L_q)}{2J_m},\ Z_{10} = \frac{L_q}{L_d},\ Z_{11} = \frac{1}{Z_{10}}.$$

Also, u_d, u_q represent the d-axis and q-axis stator voltages; i_d, i_q are the d-axis and q-axis stator currents; R_s denotes the stator resistance while L_d, L_q stand for the d-axis and q-axis stator inductances; T_e, T_L are the electromagnetic torque and load torque, respectively; J_m is the rotor inertia; B_m is the viscous friction coefficient; p signifies the number of poles; ω_r is the electrical rotor speed; and ψ_m is the magnet flux linkage.

It is assumed that the state variables (i.e., ω_r, i_d, i_q) of the system are measurable. By considering the *d–q* stator current in (1), its corresponding state-space equation in continuous-time is represented as

$$\dot{x}(t) = Ax(t) + Bu(t) + B_d\Lambda_d(t) \tag{2}$$

where

$$A = \begin{bmatrix} -Z_4 & -\omega_r Z_{10}\\ \omega_r Z_{11} & -Z_7\end{bmatrix},\quad B = \begin{bmatrix} Z_6 & 0\\ 0 & Z_8\end{bmatrix},\quad B_d = \begin{bmatrix}1\\0\end{bmatrix}.$$

$x = [i_q\ i_d]^T$ and $u = [u_q\ u_d]^T$ represent the state variable vector and control input vector in continuous-time, respectively, while $\Lambda_d(t) = -Z_5\omega_r(t)$. Now, it follows from the fact that an MPC strategy intuits the decision making of the human being in a discrete form, implying that the continuous-time model (2) should be transformed into a discrete-time model.

Using the first-order Euler's approximation method, the derivative of the *d–q* stator currents is defined as [24]

$$\frac{di_{dq}(t)}{dt} \approx \frac{i_{dq}\,(k+1) - i_{dq}\,(k)}{T_s} \tag{3}$$

where T_s is the sampling time interval. Thus, in this controller design, it is assumed that for a sampling period T_s, the control input vector $[u_q\ u_d]$ is obtained from the predicting model for the q-axis and d-axis stator current components. In that case, predicted states in the discrete-time state-space for an instant $k+1$ are given by

$$x_m\,(k+1) = A_m x_m\,(k) + B_m u_m\,(k) + B_{dm}\Lambda_d\,(k) \tag{4}$$

where

$$A_m = \begin{bmatrix} 1 - Z_4T_s & -\omega_r Z_{10}T_s\\ \omega_r Z_{11}T_s & 1 - Z_7T_s\end{bmatrix},\ B_m = \begin{bmatrix} Z_6T_s & 0\\ 0 & Z_8T_s\end{bmatrix},$$
$$B_{dm} = \begin{bmatrix} T_s\\ 0\end{bmatrix}$$

and $x_m(k)$, $x_m(k+1)$ are the state variable vectors in discrete-time at the current time step k and the next time $k+1$, respectively, whereas $u_m(k)$ is the control input vector at the current time step k. Now, (4) allows the predictions of the *d–q* stator current components which are used to predict the electromagnetic torque and stator flux linkage. Also, they determine the appropriate switching states for the three-phase IGBT voltage source inverter. In the next section, the control law based on the MP-DTC strategy and parameter update laws will be established.

B. Proposed FMP-DTC Technique Design

First, the *d–q* components of the stator flux-linkage $\psi_d(k+1)$ and $\psi_q(k+1)$ can be reconstructed based on the predicted *d–q* stator current components (4) as

$$\psi_q\,(k+1) = L_q i_q\,(k+1) \tag{5}$$
$$\psi_d\,(k+1) = L_d i_d\,(k+1) + \psi_m. \tag{6}$$

In this case, the *d–q* stator currents $i_d(k+1)$ and $i_q(k+1)$ are obtained from (4) while the *d–q* current vector $i_d(k)$ and $i_q(k)$ are determined from the measured stator current $i_{abc}(k)$ using Park's transformation. Here the rotor position angle, $\theta_r(k)$ can be obtained by using an incremental encoder. Next, the rotor speed can be calculated using the Euler's approximation method over a sampling time T_s as

$$\omega_r\,(k) = \frac{\theta_r\,(k) - \theta_r\,(k\ -\ 1)}{T_s}. \tag{7}$$

Based on the predictive *d–q* stator currents at the instant $k+1$ in (4), the magnitudes of the predicted electromagnetic torque, $T_e(k+1)$ and stator flux linkage, $\psi_s(k+1)$ are given by

$$T_e\,(k{+}1) = \frac{3}{2}p\left[\psi_m i_q\,(k{+}1){+}(L_d{-}L_q)\,i_d\,(k{+}1)\,i_q\,(k{+}1)\right] \tag{8}$$

$$\psi_s\,(k+1)\ = \sqrt{\left[\psi_q\,(k+1)\right]^2 + \left[\psi_d\,(k+1)\right]^2}. \tag{9}$$

Then the control input vector $u_m = [u_{dm}\ u_{qm}]^T$ can be selected based on the following transformation matrix:

$$u_m(k) = \frac{2}{3}V_{\rm dc}\begin{bmatrix} \cos\left(\theta_r(k)\right) & -\sin\left(\theta_r(k)\right) \\ \cos\left(\theta_r(k) - \dfrac{2\pi}{3}\right) & -\sin\left(\theta_r(k) - \dfrac{2\pi}{3}\right) \\ \cos\left(\theta_r(k) + \dfrac{2\pi}{3}\right) & -\sin\left(\theta_r(k) + \dfrac{2\pi}{3}\right) \end{bmatrix}^T \begin{bmatrix} S_a(k) \\ S_b(k) \\ S_c(k) \end{bmatrix} \tag{10}$$

where $S_{abc}(k) = [S_a(k),\, S_b(k),\, S_c(k)]^T$ is the switching vector within the eight-elements set $[0,0,0]^T$, $[0,0,1]^T$, $[0,1,0]^T$, …, $[1,1,0]^T$, $[1,1,1]^T$.

C. Fuzzy Cost Function Optimization

It is worth noting that this paper appropriately determines the weighting factors at each sampling time by introducing the fuzzy cost function in MP DTC formulation. Note that the torque and stator flux linkage predictions with their respective reference values are fed into the fuzzy cost function for the error minimization. On the other hand, to evaluate the performance of the MP DTC, the torque (ΔT_e) and stator flux ($\Delta\psi_s$) errors must be minimized. Thus, the conventional cost function $g_i(T_e,\,\psi_s)$ which minimizes the errors ΔT_e and $\Delta\psi_s$ is given as

$$g_i = \left(\|T_e^* - T_e(k+1)_i\|^2\right) + \delta_{\psi n}\left(\|\psi_s^* - \psi_s(k+1)_i\|^2\right) + C_{lim}\left\{i_s\,(k+1)\right\} \tag{11}$$

where $\delta_{\psi n}$ represents the fixed weighting factor which is computed as $\delta_{\psi n} = T_{ne}/\psi_{ns}$ in order to give the electromagnetic torque and stator flux linkage the same weight [17], [24]. In that case, T_{ne} and ψ_{ns} correspond to the nominal magnitudes of the electromagnetic torque and stator flux linkage, respectively, whereas $C_{lim}\,i(k+1)$ is the constraints function which handles the limitations of the stator current. As can be observed in (11), the fixed value of $\delta_{\psi n}$ may result in unsatisfactory performances given the dynamics of the EV traction and constraints of an IPMSM drive. Therefore, the variable weighting factors δ_T and δ_ψ are introduced in this paper whereby their values are determined online by the FLC strategy in order to appropriately select the optimal switching state $S_{abc-\rm opt}(k)$ at each sampling time, T_s. Thus, the new fuzzy cost function is established as follows:

$$\widehat{g}_i = \frac{\delta_T}{T_{ne}^2}\left(\|T_e^* - T_e(k{+}1)_i\|^2\right) + \frac{\delta_\psi}{\psi_{ns}^2}\left(\|\psi_s^* - \psi_s(k{+}1)_i\|^2\right) + C_{lim}\left\{i_s\,(k+1)\right\} \tag{12}$$

where the above references T_e^* and ψ_s^* are obtained as described in [28] and [29]. That is, T_e^* is generated from the speed loop and ψ_s^* is set based on the maximum torque per ampere (MTPA) trajectory control. Using the *d–q* flux linkage relationship, ψ_s^* is calculated as

$$\psi_s^* = \sqrt{\left(L_q i_q^*(k)\right)^2 + \left(L_d i_d^*(k) + \psi_m\right)^2} \tag{13}$$

where i_q^* corresponds to the generated T_e^* and i_d^* is obtained from the MTPA trajectory control as given by [2] and [29]. To this end, the impact of the MTPA utilization in this work is of two folds [18], [31]: 1) to increase efficiency (by minimizing copper loss); and 2) to increase torque production (by taking into account reluctance torque)

$$i_d^* = \frac{\psi_m}{2(L_q - L_d)} - \sqrt{\frac{\psi_m^2}{4(L_q - L_d)^2} + i_q^2}. \tag{14}$$

Using the prediction models (8) and (9), the *i*th element of the predicted $T_e(k+1)$ and $\psi_s(k+1)$ is determined with the corresponding switching state, $S_{abc}(k)_i$ within the eight-elements set $[0,0,0]^T$, $[0,0,1]^T$, $[0,1,0]^T$, …, $[1,1,0]^T$, $[1,1,1]^T$. To guarantee the generation of the optimal switching state $S_{abc-\rm opt}(k)$ by minimizing the cost function (12), the torque and stator flux errors should be accurately penalized at every sampling time. Therefore, by considering the two errors ($\Delta T_e = T_e^* - T_e(k+1)$, $\Delta\psi_s = \psi_s^* - \psi_s(k+1)$), the following fuzzy rules, respectively, are designed to determine the weighting factors δ_T and δ_ψ:

Fuzzy rule l for ΔT_e: IF $(\Delta T_e,\ \Delta\psi_s)$ is F_{lt}, THEN δ_T is G_{lt}.
Fuzzy rule l for $\Delta\psi_s$: IF $(\Delta T_e,\ \Delta\psi_s)$ is F_{lp}, THEN δ_ψ is G_{lp}

where $l = 1, 2, \ldots, N_r$ while N_r is the total number of the fuzzy rules, $(F_{lt},\, F_{\rm lp})$ denote the fuzzy sets associated with the errors $(\Delta T_e,\ \Delta\psi_s)$, and $(G_{lt},\ G_{\rm lp})$ are the fuzzy sets associated with the weighting factors $(\delta_T,\ \delta_\psi)$, respectively. The fuzzy sets F_{lt}, $F_{\rm lp}$, G_{lt}, and $G_{\rm lp}$ are characterized by the membership functions $g_{ltf}(\Delta T_e,\ \Delta\psi_s)$, $g_{lpf}(\Delta T_e,\ \Delta\psi_s)$, $g_{ltg}(\Delta T_e,\ \Delta\psi_s)$, and $g_{lpg}(\Delta T_e,\ \Delta\psi_s)$, respectively. In this paper, the Gaussian membership functions are selected to further characterize the fuzzy sets F_{lt}, $F_{\rm lp}$, G_{lt}, and $G_{\rm lp}$ because of their simplicity, smoothness, and nonzero properties at all points. First, the fuzzy rule sets that can generate the weighting factor δ_T for ΔT_e are given by the following.

1) IF ΔT_e is positive big (PB), THEN δ_T is PB.
2) IF ΔT_e is positive small (PS), THEN δ_T is PS.

Similar fuzzy rule sets can be applied to generate the weighting factor δ_ψ for $\Delta\psi_s$. Next, the design steps for the complete

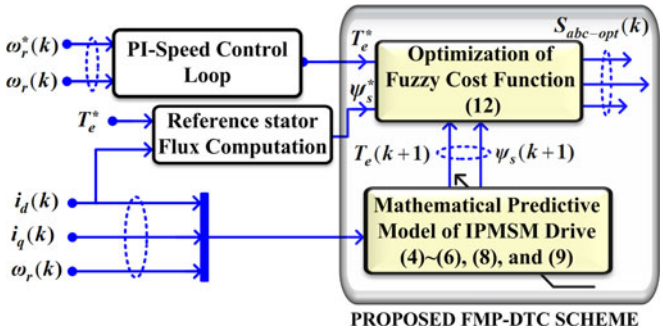


Fig. 2. Schematic diagram of the proposed FMP-DTC system for an IPMSM drive.

operation of the proposed FMP-DTC strategy can be summarized by "*Step 1 – Step 6*" below.

Step 1: Measure the stator current $i_{abc}(k)$ and rotor position $\theta_r(k)$, then determine $i_d(k)$, $i_q(k)$, and $\omega_r(k)$.

Step 2: Obtain the prediction model $i_d(k+1)$, $i_q(k+1)$, then predict $T_e(k+1)$ and $\psi_s(k+1)$ for all the possible $S_{abc}(k)$.

Step 3: Generate the references, T_e^* using the PI-speed control loop and ψ_s^* using the MTPA algorithm.

Step 4: Evaluate the cost function (12) with dynamic weighting factors (δ_T, δ_ψ) tuned by the FLC technique.

Step 5: Determine the optimal switching state, $S_{abc-\mathrm{opt}}(k)$ for driving the three-phase inverter.

Step 6: Set $k = k+1$. Go to *Step 1*.

Remark 1: The FLC strategy has been incorporated into the MP- DTC scheme to efficiently determine the weighting factors (δ_T and δ_ψ) under various dynamic conditions in torque and speed. Therefore, it can be observed that they (i.e., δ_T and δ_ψ) are directly related to the optimal control input $u_m(k)$, which is obtained as a function of the optimal switching sates (i.e., $S_a(k)$, $S_b(k)$, and $S_c(k)$). To this end, the weighting factors (δ_T and δ_ψ) are continuously updated by using the FLC technique in spite of the load torque or speed operating conditions. In this case, if the torque or flux linkage errors are large, then the fuzzy cost function (12) should highly penalize them to reduce their influence on selecting the voltage vector. Similarly, if the torque or flux linkage errors are small, the fuzzy cost function (12) should penalize them less to increase their influence on selecting the voltage vector. Note that the selected voltage vector should enforce small torque and flux errors for the optimal solution. Unlike the conventional MP-DTC, the optimal switching states of the proposed predictive torque control are selected without retuning the weighting factors. Therefore, the proposed FMP-DTC is effective in various operating conditions, which is an attractive control feature for the EV-traction applications because this has an impact on reducing the torque ripples and harmonics which are very harmful to EV drives that could result in overheat and low efficiency if they are not properly taken into account.

Fig. 2 presents the schematic diagram of the proposed FMP-DTC system for the EV traction with an IPMSM drive. Actually, the electromagnetic torque $T_e(k+1)$ and stator flux linkage

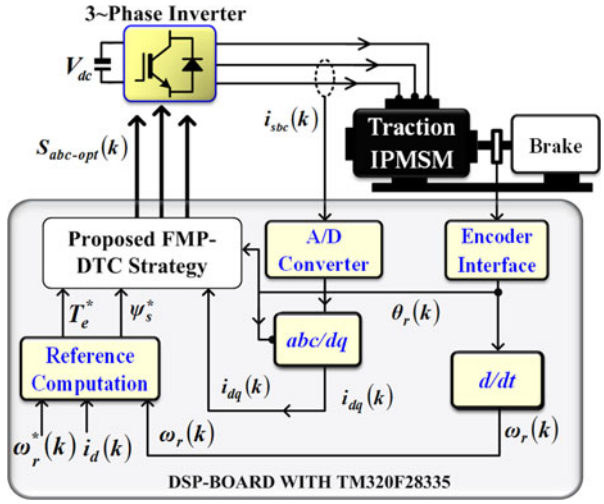


Fig. 3. Overall block diagram of a prototype IPMSM drive used in simulation and experimental studies.

$\psi_s(k+1)$ are predicted using the mathematical predictive model. Next, the optimized switching states, i.e., $S_{abc-\mathrm{opt}}(k)$ are determined by minimizing the cost function with the weighting factors, δ_T for the torque error and δ_ψ for the stator flux error.

IV. Implementation and Validation

Fig. 3 illustrates the overall block diagram of a prototype IPMSM drive used in experimental studies. In this figure, an IPMSM drive system consists of three main parts: a brake which generates the required driving torque, a three-phase IGBT inverter that provides the voltage pulses to the stator windings, and a TI TMS320F28335 DSP control board which executes the proposed FMP-DTC algorithm. The rotor position information (θ_r) is extracted using an incremental encoder RIA-40-1024ZO with 1024 pulses per revolution. Also, the stator currents (i_{sb}, i_{sc}) are detected by using the Hall-effect current sensor LTS6-NP and are converted into digital values by the 12-bit A/D converters. For each sampling time T_s, the optimal switching signals $S_{abc-\mathrm{opt}}(k)$ are determined by minimizing the fuzzy cost function (12) that includes the dynamic weighting factors, δ_T and δ_ψ. To this end, the weighting factors of the predictive torque control scheme highly influence the torque ripples for the same sampling frequency set [22]–[24]. On the other hand, the sampling time used for the comparative simulation and experimental results is 200 μs (i.e., 5 kHz). The additional fuzzy logic algorithm that has been incorporated in comparison to the conventional MP-DTC is just a piece of logic with few lines. In this case, with the advanced development of the DSP today, the proposed FMP-DTC scheme does not affect much the processing time and CPU utilization to execute the algorithm compared to the traditional MP-DTC method.

Moreover, the parameters used in simulation and experimental studies are listed as follows: stator resistance, $R_s = 2.48\,\Omega$; q-axis stator inductance, $L_q = 113.91$ mH; d-axis stator inductance, $L_d = 74.98$ mH; equivalent rotor inertia, $J_m = 0.00042\,\mathrm{kg \cdot m^2}$; viscous friction coefficient, $B_m = 0.0001\,\mathrm{N \cdot m \cdot s/rad}$; dc-link voltage, $V_{\mathrm{dc}} = 295$ V; number of poles,

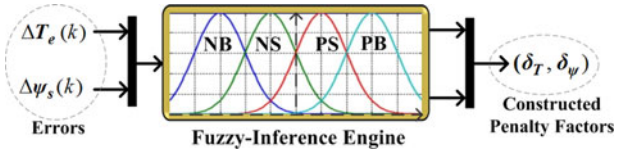


Fig. 4. Block diagram to construct the weighting factors (δ_T, δ_ψ) by the proposed fuzzy method.

$p = 4$; magnetic flux linkage, $\psi_m = 0.193\,\text{V}\cdot\text{s/ rad}$; sampling period, $T_s = 200\,\mu\text{s}$.

Thus, to reflect the real driving conditions and the constraints behaviors of the EV-traction with an IPMSM drive, the following scenarios are considered [3].

Scenario 1: Steady-state operation (i.e., EV cruising with constant speed) at constant load torque.

Scenario 2: Rapid speed change (i.e., EV overtaking or braking in emergency) at constant load torque.

Scenario 3: Load torque step change (i.e., EV sudden climbing or descending) at constant speed.

Fig. 4 indicates the implementation of the fuzzy method to construct the two weighting factors (δ_T, δ_ψ) from ΔT_e and $\Delta\psi_s$. In this case, the total number of rules for each weighting factor is set as $N_r = 4$ directly based on the number of input (ΔT_e) and output (δ_T) in relation to the selected linguistic values (PS, PB, etc.). Then, the following membership functions are used to characterize the fuzzy sets F_{lt}, F_{lp}, G_{lt}, and G_{lp} for $l = 1, \ldots, 4$:

$$g_{1tf}(\Delta T_e, \Delta\psi_s) = g_{1tg}(\Delta T_e, \Delta\psi_s) = e^{-(\Delta T_e+2)^2/2^2},$$

$$g_{2tf}(\Delta T_e, \Delta\psi_s) = g_{2tg}(\Delta T_e, \Delta\psi_s) = e^{-(\Delta T_e+0.1)^2/0.1^2},$$

$$g_{3tf}(\Delta T_e, \Delta\psi_s) = g_{3tg}(\Delta T_e, \Delta\psi_s) = e^{-(\Delta T_e-0.1)^2/0.1^2},$$

$$g_{4tf}(\Delta T_e, \Delta\psi_s) = g_{4tg}(\Delta T_e, \Delta\psi_s) = e^{-(\Delta T_e-2)^2/2^2},$$

$$g_{1pf}(\Delta T_e, \Delta\psi_s) = g_{1pg}(\Delta T_e, \Delta\psi_s) = e^{-(\Delta\psi_s+0.5)^2/0.5^2},$$

$$g_{2pf}(\Delta T_e, \Delta\psi_s) = g_{2pg}(\Delta T_e, \Delta\psi_s) = e^{-(\Delta\psi_s+0.01)^2/0.01^2},$$

$$g_{3pf}(\Delta T_e, \Delta\psi_s) = g_{3pg}(\Delta T_e, \Delta\psi_s) = e^{-(\Delta\psi_s-0.01)^2/0.01^2},$$

$$g_{4pf}(\Delta T_e, \Delta\psi_s) = g_{4pg}(\Delta T_e, \Delta\psi_s) = e^{-(\Delta\psi_s-0.5)^2/0.5^2}.$$

Note that, the operating points are selected based on the nominal values of the electromagnetic torque and stator flux linkage with some small tolerance. The advantages of the proposed scheme include the following: high performance of torque control (i.e., faster torque response and low ripples) at wide operating range and simple implementation compared to the conventional DTC schemes. Also, the optimal switching states of the proposed FMP-DTC are obtained without retuning the weighting factors irrespective of the operating conditions, which are not trivial for the conventional MP-DTC [24]. On the other hand, the limitation of the proposed scheme is the delay compensation that is needed during implementation. Nevertheless, this problem has been widely studied in digital implementation and reported in existing MPC literatures [18]–[20], [24]. Meanwhile, the main disadvantage of the proposed FMP-DTC scheme is the increase in execution time compared to the conventional MP-DTC. This is due to the inclusion of a fuzzy logic algorithm to improve the system performance as explained earlier. However, it poses less challenge for the contemporary DSP experimental performance and implementation because most complex algorithms like fuzzy, neural network or extended Kalman filter are widely found in commercial off-the-shelf products [27], [28]. And there is always a room to efficiently reduce the algorithm complexity in real-time implementation for industrial products [32].

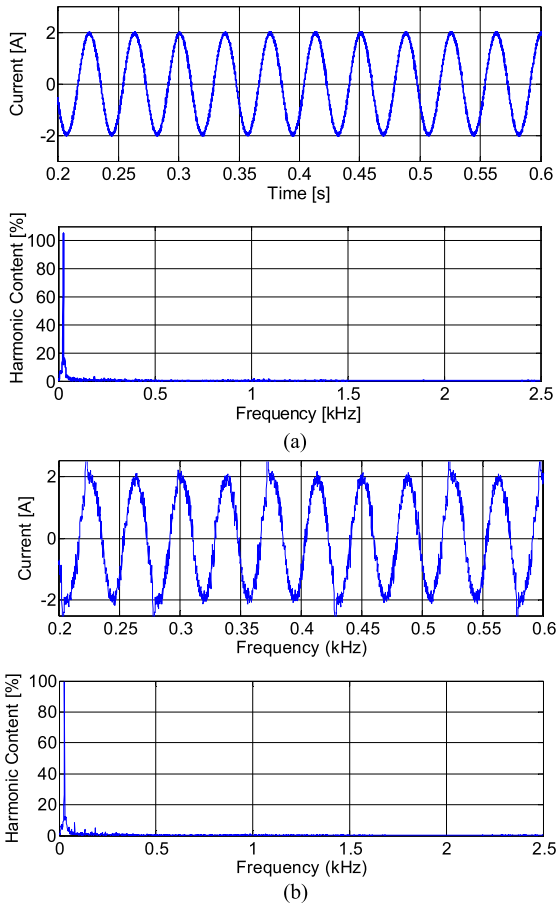


Fig. 5. Simulation results of the proposed FMP-DTC strategy under *Scenario 1* (i.e., steady-state performance): phase *a* stator current and its corresponding frequency spectrum. (a) Proposed FMP-DTC strategy. (b) Conventional MP-DTC strategy.

A. Simulation Results

Examining the driving condition of the steady-state operation under *Scenario 1* (i.e., EV cruising with constant speed), the desired speed of the IPMSM drive is set to $\omega_r^* = 167.5\,\text{rad/s}$ at constant load torque, $T_L = 1.2\,\text{N}\cdot\text{m}$. Fig. 5(a) and (b) shows the phase *a* stator current waveform and its corresponding frequency spectrum under *Scenario 1*, for the proposed FMP-DTC and conventional MP-DTC schemes, respectively. This steady-state performance is presented to assess the stator current quality under the proposed FMP-DTC when compared to the

conventional MP-DTC in terms of the harmonic contents. In this figure, the harmonic contents are presented as the percentages of the fundamental current magnitude. In this scenario, the fundamental frequency of the stator current components is 26.7 Hz. Based on the frequency spectrum shown in Fig. 5(a), the significant harmonic components in phase a are found to be 5th, 7th, and 11th with the magnitudes of 2.9%, 2.1%, and 1.1%, respectively. On the other hand, the harmonic contents for the conventional MP-DTC revealed in Fig. 5(b) are 3.8%, 3.4%, and 1.9%, respectively. There is increased in harmonic contents for the conventional MP-DTC as shown in Fig. 5(b) due to a poor ability of the MP-DTC technique to mitigate the ripples. Nonetheless, since both control methods inherently possess variable switching frequency characteristics, it is known that the frequency components above Shannon or Nyquist frequency (i.e., 2.5 kHz in this case) are removed as the switching frequency is limited to this value (i.e., Nyquist frequency). Hence, the harmonic contents appear below this frequency (2.5 kHz) as shown in Fig. 5. It should be noted that these harmonics result in total harmonic distortion which is acceptable in industrial applications [30].

Next, Fig. 6 shows the comparative simulation results about the speed transient performances of both the proposed FMP-DTC and conventional MP-DTC strategies under *Scenario 2* (i.e., overtaking situation). In this figure, the following waveforms are presented: the speed reference (ω_r^*), measured speed (ω_r), generated electromagnetic torque (T_e), electromagnetic torque reference (T_e^*), stator flux linkage (ψ_s), stator flux linkage reference (ψ_s^*), and d–q stator current components (i_d, i_q). Under this scenario, the speed trajectory is abruptly changed from $\omega_r^* = 104.5$ rad/s to $\omega_r^* = 313.5$ rad/s at a constant load torque, $T_L = 1.2\,\mathrm{N}\cdot\mathrm{m}$. Now, as depicted in Fig. 6(a) and (c), the proposed FMP-DTC scheme precisely tracks the speed trajectory with shorter settling time and no oscillations than the conventional MP-DTC scheme because of the newly introduced weighting factors tuned by the FLC technique. In particular, Fig. 6(b) shows the waveforms of the dynamic weighting factors (δ_T and δ_ψ) under this condition for the proposed FMP-DTC scheme. As shown in Fig. 6(b), the weighting factors are continuously changing to offset the torque and flux errors that influence the optimal selection of the switching states. Considering the dynamic behaviors, the proposed FMP-DTC scheme has far more improved responses than the conventional MP-DTC scheme, i.e., overshoot (5.2%/23.5%) and the settling time (110 ms/260 ms) without the steady-state speed errors.

Finally, the torque transient behaviors of the proposed DTC method and the conventional DTC method are again investigated under *Scenario 3* (i.e., rapid climbing mode) as depicted in Fig. 7. In this case, the load torque is suddenly changed from 0.5 to 1.2 Nċm at constant speed trajectory of $\omega_r^* = 251.3$ rad/s. Fig. 7(a) and (c) presents the simulation results of the proposed FMP-DTC scheme and the conventional MP-DTC scheme under this scenario, respectively. Also, Fig. 7(b) reveals the waveforms of the dynamic weighting factors corresponding to a load torque step change. It is clearly observed from Fig. 7(a) and (c) that the proposed control scheme quickly converges to its commanded speed with little overshoot regardless of

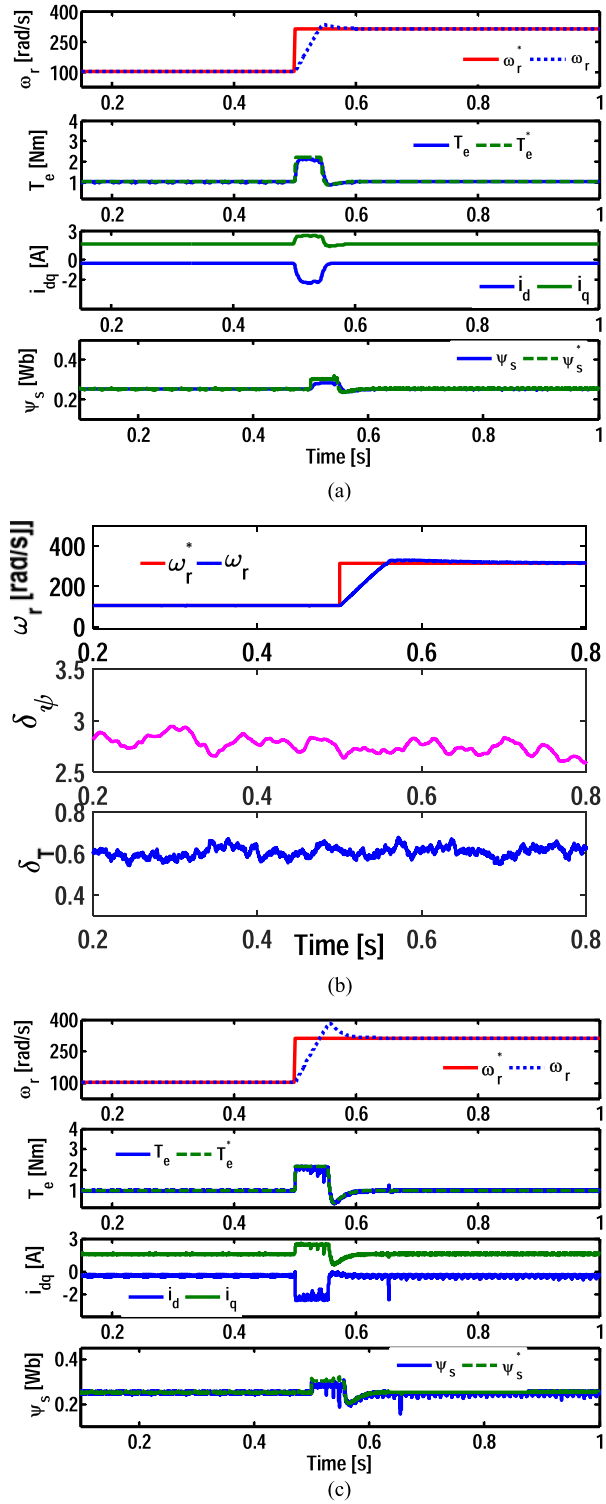


Fig. 6. Simulation results under *Scenario 2* (i.e., overtaking situation). (a) Proposed FMP-DTC strategy. (b) Dynamic weighting factors of the proposed FMP-DTC strategy. (c) Conventional MP-DTC strategy.

the sudden load torque change. This is due to the fact that the dynamic weighting factors cancel out the offsets caused by the sudden load torque changes, leading to lower ripples and overshoots in torque and stator flux during transient-state compared to the conventional MP-DTC scheme. To be more

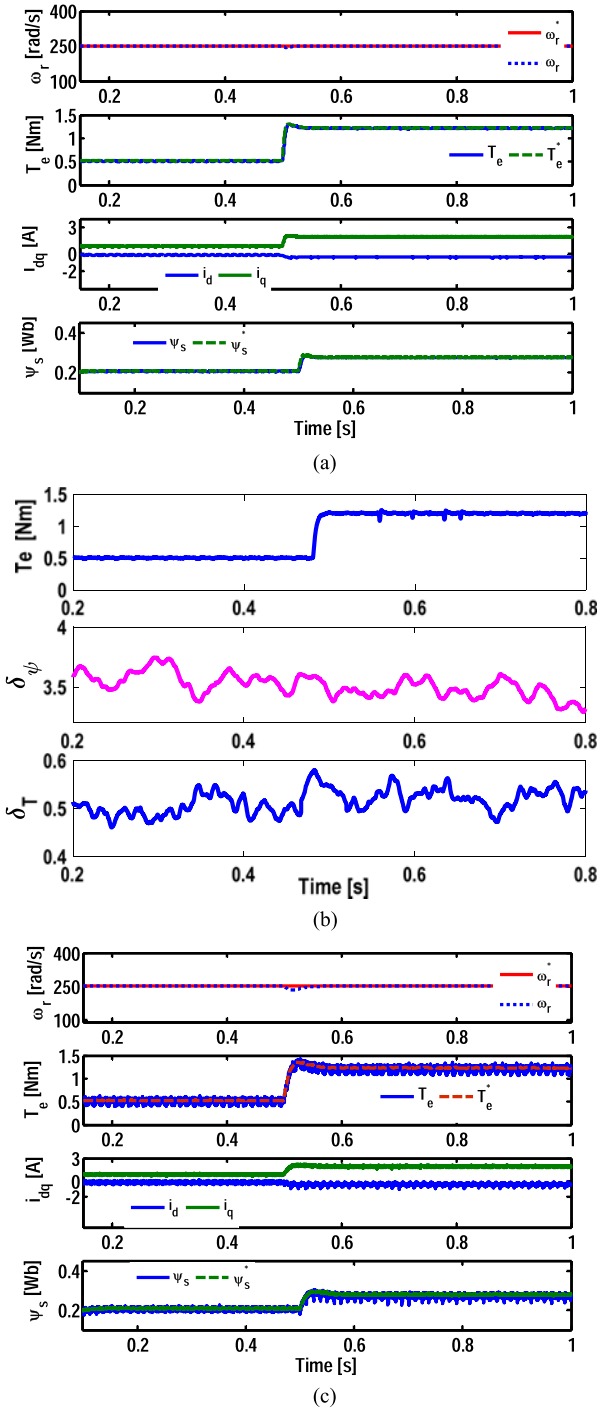


Fig. 7. Simulation results under *Scenario 3* (i.e., sudden climbing condition). (a) Proposed FMP-DTC strategy. (b) Dynamic weighting factors of the proposed FMP-DTC strategy. (c) Conventional MP-DTC strategy.

specific, the proposed FMP-DTC has smoother responses in all displayed parameters in comparison with the conventional MP-DTC. Thus, the quantitative comparisons between the proposed and conventional schemes during the transient-state are: overshoot (1.2%/13.5%) and the settling time (2 ms/ 20 ms). In addition, Fig. 8 displays the comparative results of the proposed FMP-DTC and the conventional MP-DTC with respect to the torque and stator flux during transient-state under *Scenario 3*.

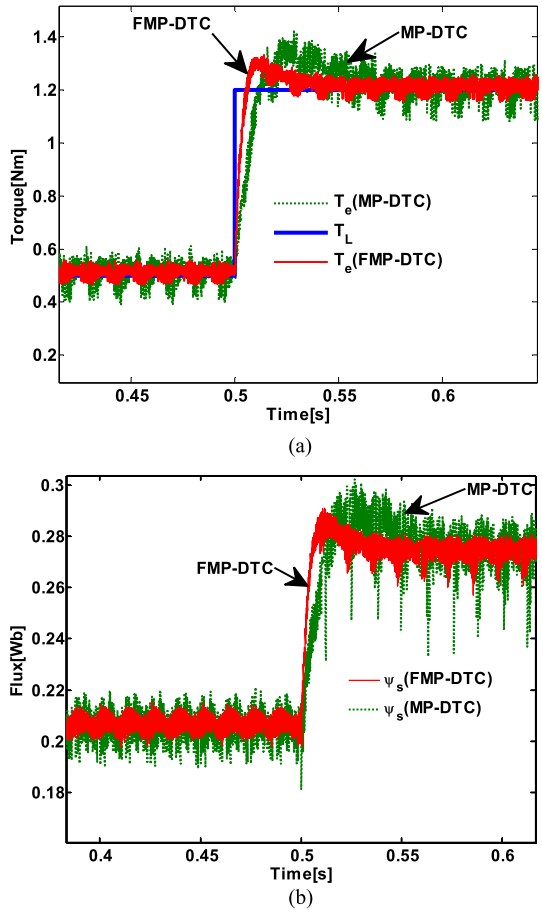


Fig. 8. Comparative simulation results under *Scenario 3*. (a) Electromagnetic torque responses. (b) Stator flux responses.

It can be apparently seen that the torque and flux ripples are highly reduced with the proposed FMP-DTC compared to the conventional MP-DTC. It is also worth mentioning that the salient feature of the proposed scheme is its ability to reduce the ripples which might propagate oscillations in the torque that could lead to vibrations in the mechanical systems.

B. Experimental Results

An experimental setup is designed to further validate the performance of the proposed FMP-DTC scheme and the results are compared with those of the conventional MP-DTC scheme. The studies are carried out while considering the same *Scenarios 1–3* as those used in the simulation studies. First, the harmonic components of the stator current are investigated under steady-state condition (*Scenario 1*). The IPMSM drive is ran with a constant speed trajectory of 167.5 rad/ s at constant load torque of $T_L = 1.2\,\mathrm{N}\cdot\mathrm{m}$. The fundamental frequency of this waveform can be computed as 26.7 Hz. The spectrum analysis of the stator current is accomplished by using Tektronix TDS5000-series digital oscilloscope with a sampling rate set to 50 kHz. The phase *a* stator current and its corresponding frequency spectrum are presented in Fig. 9(a) and (b) for the proposed FMP-DTC and the conventional MP-DTC, respectively. Based on the

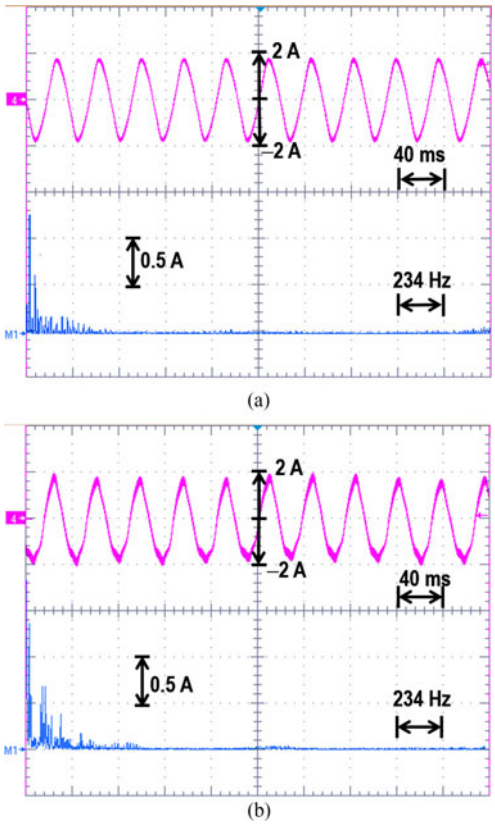


Fig. 9. Experimental results of the proposed FMP-DTC strategy under *Scenario 1* (steady-state condition): phase *a* stator current and its corresponding frequency spectrum. (a) Proposed FMP-DTC strategy. (b) Conventional MP-DTC strategy.

waveforms shown in Fig. 9, the significant harmonic components are found to be below 468 Hz, which are 5th, 7th, and 11th components. With reference to Fig. 9(a), their harmonic contents obtained based on the fundamental current magnitude are 3.2%, 2.2%, and 1.6%, respectively. In comparison, the harmonic contents obtained with respect to the conventional MP-DTC scheme shown in Fig. 9(b) are 4.3%, 3.8%, and 2.1%, respectively. It can be observed that there is a significant reduction in harmonic contents due to the ripple mitigation achieved with the proposed FMP-DTC scheme as exemplified in the previous sections. Note that the harmonics obtained are a bit higher than those obtained in the simulation studies due to some limitation such as the discrepancy in physical motor parameters. It is evident that the quality of the stator current based on the proposed FMP-DTC is within an acceptable range [30]. Besides, the time spent for executing the proposed FMP-DTC algorithm is 39.43 μs in comparison to 22.67 μs of the conventional MP-DTC algorithm. There is a small increase in execution time of 42.5% with the proposed FMP-DTC scheme due to the inclusion of a fuzzy logic algorithm, but the performance is better with little expense in time [21]. It is worth to stress that the proposed FMP-DTC still can be implemented using general DSP chips widely used in the industry.

Furthermore, the speed trajectory of the IPMSM drive at 104.5 rad/s is rapidly changed to 313.5 rad/s while a constant

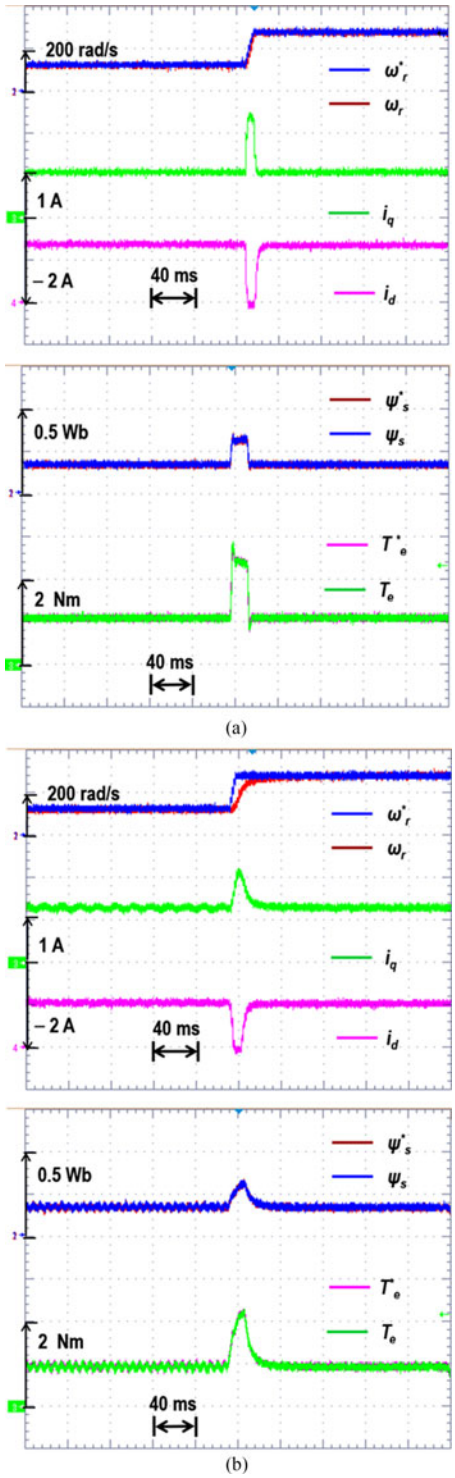


Fig. 10. Experimental results under *Scenario 2* (i.e., overtaking situation). (a) Proposed FMP-DTC strategy. (b) Conventional MP-DTC strategy.

load torque, $T_L = 1.2\,\mathrm{N}\cdot\mathrm{m}$ is applied to validate the dynamic performance of the proposed controller (*Scenario 2*). From the transient responses indicated in Fig. 10(a), the proposed FMP-DTC strategy can still show excellent speed tracking performances with shorter settling times for the torque (20 ms) and stator flux (20 ms), whereas it shows no significant overshoots

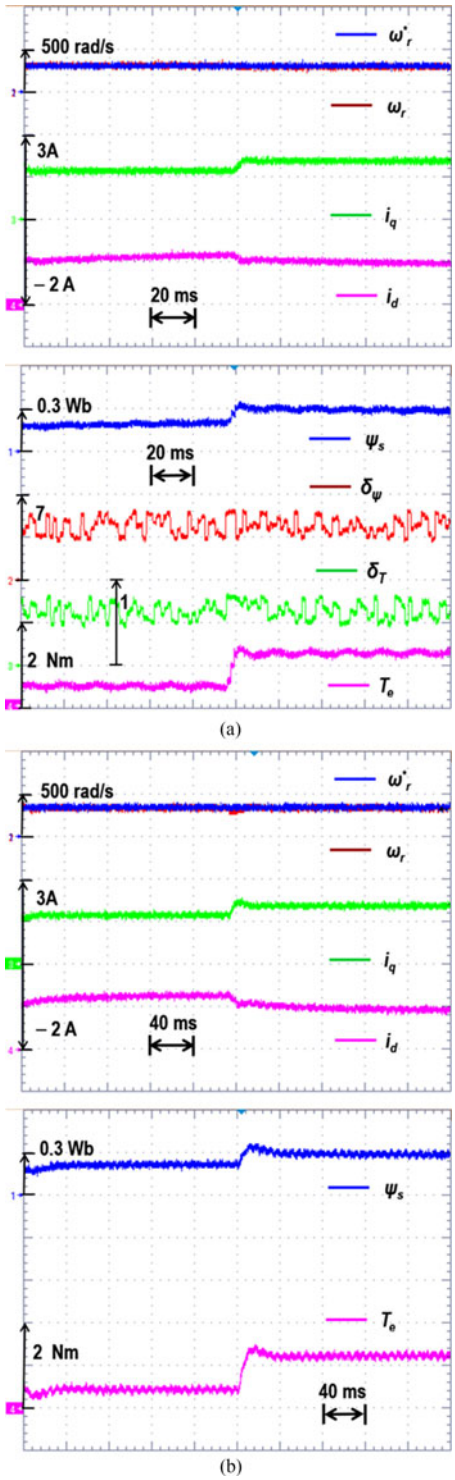


Fig. 11. Experimental results under *Scenario 3* (i.e., sudden climbing condition). (a) Proposed FMP-DTC strategy. (b) Conventional MP-DTC strategy.

as shown in Fig. 10(a). In the conventional MP-DTC, the corresponding settling times are 30 and 60 ms while its overshoots as shown in Fig. 10(b) are 11.3% and 17.6% for the torque and stator flux linkage, respectively. Fig. 10(b) also reveals large ripples (21.5%) in comparison to the proposed FMP-DTC (0.7%) in Fig. 10(a).

Finally, the third experimental study (*Scenario 3*) is carried out to investigate the sudden load torque perturbations (from 0.5 to 1.2 N·m) response when the speed trajectory is maintained at 251.3 rad/s. Fig. 11 shows the comparative experimental results under *Scenario 3*. Thus, as can be observed in Fig. 11(a), the proposed FMP-DTC scheme indicates that the speed response is almost the same as its commanded speed. Moreover, the transient responses of the torque and stator flux have shorter settling times (3 ms/ 5 ms) and almost no oscillations compared to the conventional MP-DTC scheme. Also, Fig. 11(a) includes the weighting factors (δ_ψ, δ_T) to expose their contributions in the proposed FMP-DTC scheme. The tracking errors of the torque and flux responses are counter-balanced to give the possible fastest response. It is important to note that 20 ms/div. is used in comparison to 40 ms/div. in Fig. 11(b) to identify in detail the weighting factors responses in relation to the instantaneous torque and flux quantities. Alternatively, the performances of the conventional MP-DTC scheme presented in Fig. 11(b) for the torque and stator flux have longer settling times (10 ms/30 ms) and much more oscillations in both responses.

V. Conclusion

This paper presents a FMP-DTC strategy for the EV-traction with an IPMSM drive. By using the embedded online fuzzy logic tuning algorithm, the dynamic weighting factors are generated which enhance the performance of the proposed FMP-DTC scheme. Thus, the proposed scheme can precisely track the speed trajectory and guarantee a high performance even during the speed transients (i.e., normal and rapid climbing) or load torque step change (i.e., sudden climbing or emergency braking) which are similar to the EV-traction operations. From the simulation and experimental studies, the proposed FMP-DTC scheme demonstrated a fast speed tracking and precise torque response when compared to the conventional MP-DTC scheme. It was apparently observed that the proposed FMP-DTC produced the low torque and stator flux ripples in both scenarios in comparison with the conventional MP-DTC. Apart from making automatically an optimal tradeoff between the equally important torque and flux errors by using a fuzzy cost function, the proposed FMP-DTC scheme has a simple structure and preserves the advantages of the basic DTC scheme. Even though the proposed scheme was designed and presented in the sense that the torque and flux ripples are significantly reduced, it will be extended to consider the system robustness against parameters change and EV-traction dynamics with a real EV traction motor drive, which are interesting further research issues. In this paper, the EV traction drive has been considered as a general case for the systems that require the DTC. However, this proposed method can be easily applied to other electromechanical or mechatronics systems like CNC machines without significant modification.

References

[1] M. A. Rahman, M. A. Masrur, and M. N. Uddin, "Impacts of interior permanent magnet machine technology for electric vehicles," in *Proc. IEEE Int. Elect. Veh. Conf.*, 2012, pp. 1–5.

[2] D. Q. Dang, N. T. T. Vu, H. H. Choi, and J. W. Jung, "Neuro-fuzzy control of interior permanent magnet synchronous motors: Stability analysis and implementation," *J. Elect. Eng. Technol.*, vol. 8, no. 6, pp. 1439–1450, Nov. 2013.
[3] M. E. H. Benbouzid, D. Diallo, and M. Zeraouila, "Advanced fault tolerant control of induction-motor drives for EV/HEV traction applications: From conventional to modern and intelligent control techniques," *IEEE Trans. Veh. Technol.*, vol. 56, no. 2, pp. 519–528, Mar. 2007.
[4] A. K. Jain and V. T. Ranganathan, "Modeling and field oriented control of salient pole wound field synchronous machine in stator flux coordinates," *IEEE Trans. Ind. Electron.*, vol. 58, no. 3, pp. 960–970, Mar. 2011.
[5] O. Wallmark, S. Lundberg, and M. Bongiorno, "Input admittance expressions for field-oriented controlled salient PMSM drives," *IEEE Trans. Power Electron.*, vol. 27, no. 3, pp. 1514–1520, Mar. 2012.
[6] Y. A. R. I. Mohamed, "A newly designed instantaneous-torque control of direct-drive PMSM servo actuator with improved torque estimation and control characteristics," *IEEE Trans. Ind. Electron.*, vol. 54, no. 5, pp. 2864–2873, Sep. 2007.
[7] Y. Zhang and J. Zhu, "Direct torque control of permanent magnet synchronous motor with reduced torque ripple and commutation frequency," *IEEE Trans. Power Electron.*, vol. 26, no. 1, pp. 235–248, Jan. 2011.
[8] C. Xia, J. Zhao, Y. Yan, and T. Shi, "A novel direct torque control and flux control method of matrix converter-fed PMSM drives," *IEEE Trans. Power Electron.*, vol. 29, no. 10, pp. 5417–5430, Oct. 2014.
[9] K. Gulez, A. A. Adam, and H. Pastaci, "A novel direct torque control algorithm for IPMSM with minimum harmonic and torque ripples," *IEEE/ASME Trans. Mechatronics*, vol. 12, no. 2, pp. 223–227, Apr. 2007.
[10] Y. Zhang and J. Zhu, "A novel duty cycle control strategy to reduce both torque and flux ripples for DTC of permanent magnet synchronous motor drives with switching frequency reduction," *IEEE Trans. Power Electron.*, vol. 26, no. 10, pp. 3055–3067, Oct. 2011.
[11] Y. Cho, K. B Lee, J. H. Song, and Y. Lee, "Torque-ripple minimization and fast dynamic scheme for torque predictive control of permanent-magnet synchronous motors," *IEEE Trans. Power Electron.*, vol. 30, no. 4, pp. 2182–2190, Apr. 2015.
[12] Y. S. Choi, H. H. Choi, and J. W. Jung, "Feedback linearization direct torque control with reduced torque and flux ripples for IPMSM drives," *IEEE Trans. Power Electron.*, vol. 31, no. 5, pp. 3728–3737, May 2016.
[13] K. B. Lee and F. Blaabjerg, "Sensorless DTC-SVM for induction motor driven by a matrix converter using a parameter estimation strategy," *IEEE Trans. Ind. Electron*, vol. 55, no. 2, pp. 512–521, Feb. 2008.
[14] J. S. Lee, C. H. Choi, J. K. Seok, and R. D. Lorenz, "Deadbeat-direct torque and flux control of interior permanent magnet synchronous machines with discrete time stator current and stator flux linkage observer," *IEEE Trans. Ind. Appl.*, vol. 47, no. 4, pp. 1749–1958, Jul./Aug. 2011.
[15] G. H. B. Foo and M. F. Rahman, "Direct torque control of an IP-synchronous motor drive at very low speed using a sliding-mode stator flux observer," *IEEE Trans. Power Electron.*, vol. 25, no. 4, pp. 933–942, Apr. 2010.
[16] T. D. Do, H. H. Choi, and J. W. Jung, "Nonlinear optimal DTC design and stability analysis for interior permanent magnet synchronous motor drives," *IEEE/ASME Trans. Mechatronics*, vol. 20, no. 6, pp. 2716–2725, Apr. 2015.
[17] R. Sultana and S. K. Sahoo, "Finite control set model predictive current control for a cascaded multilevel inverter," *J. Electr .Eng. Technol.*, vol. 11, no. 6, pp. 1674–1683, Nov. 2016.
[18] M. Preindl and S. Bolognani, "Model predictive direct torque control with finite control set for PMSM drive systems, part I: Maximum torque per ampere operation," *IEEE Trans. Ind. Informat.*, vol. 9, no. 4, pp. 1912–1921, Nov. 2013.
[19] M. Preindl and S. Bolognani, "Model predictive direct torque control with finite control set for PMSM drive systems, part 2: field weakening operation," *IEEE Trans. Ind. Informat.*, vol. 9, no. 2, pp. 648–657, May 2013.
[20] P. Cortes, M. P. Kazmierkowski, R. M. Kennel, D. E. Quevedo, and J. Rodriguez, "Predictive control in power electronics and drives," *IEEE Trans. Ind. Electron.*, vol. 55, no. 12, pp. 4312–4324, Dec. 2008.
[21] C. A. Rojas, J. Rodriguez, F. Villarroel, J. R. Espinoza, C. A. Silva, and M. Trincado, "Predictive torque and flux control without weighting factors," *IEEE Trans. Ind. Electron.*, vol. 60, no. 2, pp. 681–690, Feb. 2013.
[22] Y. Zhang and H. Yang, "Two-vector-based model predictive torque control without weighting factors for induction motor drives," *IEEE Trans. Power Electron.*, vol. 31, no. 2, pp. 1381–1390, Feb. 2016.
[23] F. Villarroel, J. R. Espinoza, C. A. Rojas, J. Rodriguez, M. Rivera, and D. Sbarbaro, "Multiobjective switching state selector for finite-states model predictive control based on fuzzy decision making in a matrix converter," *IEEE Trans. Ind. Electron.*, vol. 60, no. 2, pp. 589–599, Feb. 2013.
[24] J. Rodriguez and P. Cortes, *Predictive Control of Power Converters and Electrical Drives*, Hoboken, NJ, USA: Wiley, 2012.
[25] S. Li, K. Li, R. Rajamani, and J. Wang, "Model predictive multi-objective vehicular adaptive cruise control," *IEEE Trans. Control Syst. Technol.*, vol. 19, no. 3, pp. 556–566, May 2011.
[26] G. F. H. Beng, X. Zhang, and D. M. Vilathgamuwa, "Sensor fault-resilient control of interior permanent magnet synchronous motor drives," *IEEE/ASME Trans. Mechatronics*, vol. 20, no. 2, pp. 855–864, Apr. 2014.
[27] F. Mwasilu and J. W. Jung, "Enhanced fault-tolerant control of interior PMSMs based on an adaptive EKF for EV traction application," *IEEE Trans. Power Electron.*, vol. 31, no. 8, pp. 5746–5758, Aug. 2016.
[28] P. Vas, *Sensorless Vector and Direct Torque Control*. Oxford, U.K.: Oxford Univ. Press, 1998.
[29] Y. Inoue, S. Morimoto, and M. Sanada, "Control method suitable for direct-torque-control-based motor drive system satisfying voltage and current limitations," *IEEE Trans. Ind. Appl.*, vol. 48, no. 3, pp. 970–976, May/Jun. 2012.
[30] Recommended practices and requirements for harmonic control in electrical systems, IEEE Standard, 519-1992, 1993.
[31] M. N. Uddin and R. S. Rebeiro, "Online efficiency optimization of a fuzzy-logic-controller-based IPMSM drive," *IEEE Trans. Ind. Appl.*, vol. 47, no. 2, pp. 1043–1050, Mar./Apr. 2011.
[32] T. H. Cormen, C. E. Leiserson, and R. L. Rivest, *Introduction to Algorithms*, Cambridge, MA, USA: MIT Press, 2001.



Jackson John Justo received the B.S. degree in electrical engineering from the University of Dar es Salaam, Dar es Salaam, Tanzania, in 2008, and the Ph.D. degree in electronics and electrical engineering from Dongguk University, Seoul, South Korea, in 2015.

He is currently working as a Lecturer with the Department of Electrical Engineering, University of Dar es Salaam. Since April 2016, he has been a Research Fellow with the Department of Electrical, Electronic, and Computer Engineering, University of Pretoria, Pretoria, South Africa. His current research interests include energy efficiency and management for smart city and transportation, power converter control for electric vehicles and drives, smart grid with renewable energy, energy storage systems, and simulation using real-time digital simulators and Parallel Computer Applications, Real-Time Software units.



Francis Mwasilu received the B.S. degree in electrical engineering from the University of Dar es Salaam, Dar es salaam, Tanzania, in 2008, and the Ph.D. degree in electronics and electrical engineering from Dongguk University, Seoul, South Korea, in 2016.

From 2008 to 2009, he was an Instrumentation Engineer at Illovo Sugar Ltd, Tanzania. From 2009 to 2011, he was a Utilities Engineer at Japan Tobacco International, Tanzania. Since July 2016, he has been a Lecturer with the Department of Electrical Engineering, University of Dar es Salaam. He is currently a Postdoctoral Research Fellow with the Division of Electronics and Electrical Engineering, Dongguk University. His current research interests include digital signal processor-based electric machine drives, electric vehicles, smart grid enabling technologies, and renewable energy sources integration into modern power systems.



Eun-Kyung Kim received the B.S. degree in electrical engineering from Dongguk University, Seoul, South Korea, in 2009, where she is currently working toward the Ph.D. degree in the Division of Electronics and Electrical Engineering.

From 2009 to 2012, she was at the Electrical Vehicle Research Laboratory, VCTech Company, Ltd., Gyeonggi, South Korea. Her current research interests include digital signal processor-based electric machine drives, electric vehicles, smart grid enabling technologies, and control of distributed generation systems using renewable energy sources.



Jinuk Kim received the B.S. degree in electronic engineering from Dongguk University, Seoul, South Korea, in 2014, where he is currently working toward the Ph.D. degree in the Division of Electronics and Electrical.

His current research interests include microprocessor-based electric machine drives, control of distributed generation systems using renewable energy sources, and power conversion systems and drives for electric vehicles.



Han Ho Choi (M'03) received the B.S. degree in control and instrumentation engineering from Seoul National University, Seoul, South Korea, in 1988, and the M.S. and Ph.D. degrees in electrical engineering from the Korea Advanced Institute of Science and Technology, Daejeon, South Korea, in 1990 and 1994, respectively.

He is currently with the Division of Electronics and Electrical Engineering, Dongguk University, Seoul. His current research interests include control theory and its application to real-world problems.



Jin-Woo Jung (M'06) received the B.S. and M.S. degrees in electrical engineering from Hanyang University, Seoul, South Korea, in 1991 and 1997, respectively, and the Ph.D. degree in electrical and computer engineering from Ohio State University, Columbus, OH, USA, in 2005.

From 1997 to 2000, he was at the Home Appliance Research Laboratory, LG Electronics Co., Ltd., Seoul. From 2005 to 2008, he was a Senior Engineer at the Research and Development Center and the Plasma Display Panel Development Team, Samsung SDI Co., Ltd., South Korea. Since 2008, he has been a Professor with the Division of Electronics and Electrical Engineering, Dongguk University, Seoul. His current research interests include digital signal processor-based electric machine drives, distributed generation systems using renewable energy sources, and power conversion systems and drives for electric vehicles.